Indian Journal of Engineering & Materials Sciences
Vol. 28, April 2021 pp. 189-197

Influence of B_4C on microstructural, mechanical and wear properties of Mg-based composite by two-step stir casting

Sakshi Singh* & Nathi Ram Chauhan

Mechanical and Automation Engineering Department of Indira Gandhi Delhi Technical University for Women, Delhi 110 006, India

Received: 12 May 2020; Accepted: 24 February 2021

This paper has been focused on the porosity, hardness, tensile and abrasion wear of Mg-based B_4C composites developed by squeezed vacuum-based stir casting (SVSC) process by adding 3, 5, 7, 9 wt. % of B_4C. Also, an electromagnetic stir casting has been used to synthesize similar composition specimens in comparison to the SVSC results. Additionally, electron microscopy has been used for analyzing the micro structural, fractographic and worn images of Mg-based B_4C composites and to validate appropriate fabrication method. A tribo-test has been carried out by two-body abrasion condition at 20N and 30N load for as sliding distance of 100m and 5m/s of speed. The results reveal that the SVSC process produces homogeneously distributed B_4C particles in Mg-matrix as compared to the electromagnetic stirring. The mechanical properties of Mg/B_4C composites show their significant enhancement with the addition of B_4C content in Mg-matrix. B_4C composites show an increment of 33-48% of hardness as compared to Mg-matrix. Mg-matrix having 9 wt. % of B_4C composite reveals the least tensile strength and fractured images show the cleavage planes, micro voids as well as micro cracks. Although, worn images shows oxidation and ploughing mechanism with the increase in load and depth of penetration in Mg-matrix B_4C composites.

Keywords: Mg composites, Squeezed pressure, Tensile, Microstructure, Abrasive wear

1 Introduction

The aircraft and automotive applications have been a demand in the distinct light-weight parts such as steering column parts, seat frame, and instrument panel for the automotive sector and parcel tray, headliner, and dashboard covers in aircraft design industries[1-3]. At present, such materials have been developed from Mg/Al-based composites which can be modified by reinforcing hard material as particulates or fibres. Such materials have been developed with different fabrication methods such as extrusion, powder metallurgy, mechanical alloying, and stir casting etc., which enhances and modify the properties of Mg-based composites[4,5]. In future, the heavier iron or steel materials have been replaced by composite materials for better abilities such as high efficiency, weight reduction and low fuel consumption. These materials should satisfy the favorable ultimate strength, density, thermal expansion and wear-resistant properties[6, 7].

There are different processing methods for synthesizing Mg-based parts. However feasible processing method helps to modify the phases and microstructure by the addition of different hard reinforcing material(s). This results in the proper amalgamation of reinforced particles with minimum defects in the fabricated composites.

For a decade, electromagnetic stirring (ES) has been one of the new approaches to developing Mg-based composites (Fig. 1a)[8]. This technique includes heating matrix material in a separate crucible and preheated upto molten stage. Then melt has been put into the muffle furnace of electromagnetic stirring setup. Then current and voltage have been provided to the set-up through an induction motor (3-phase) to induce the stirring action. This process has been operated by the control panel attached to the setup. The control panel records the stirring speed, voltage, current, temperature of the muffle furnace, the temperature of the melt. Continuously, argon gas has been applied to the furnace to protect from fire extinguishing. Under regulated temperature, the molten melt has been continuously stirred at a specified speed with the help of a stirrer blade. The melt rotates continuously by electro-magnetic field until solidification has been achieved. Reinforcement has been pre-heated in an electric oven to remove the moisture contents. However, the literature review

*Corresponding author (E-mail: singh.sakshi0408@gmail.com)

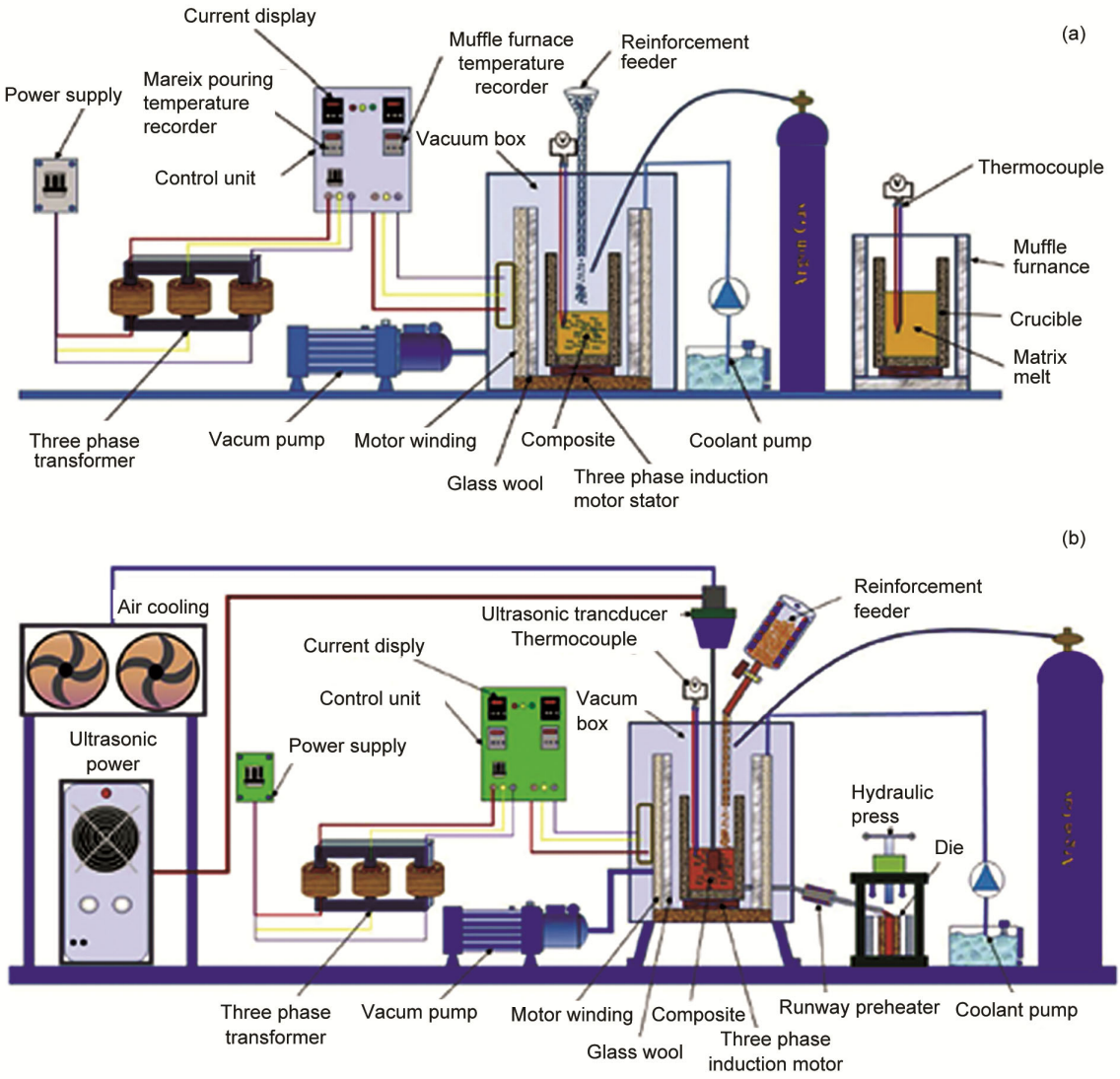

Fig. 1 — Stir casting process setup (a) electromagnetic stirring and (b) squeezed vacuum-based stir casting[8].

reported mainly on the different stir casting approaches of Mg-based composites while very few studies have been reported onsqueezed vacuum stir casting (SVSC) of Mg-based composites[9,10].

Reinforced material, boron carbide is a dark grey metallic lustre crystalline compound of carbon and boron[11]. It has positive properties such as low density with a high melting point. It is composed of icosahedrons borides and carbon atoms with strong bonds in the lattice. B_4C is not attacked by any molten salts and alkalis up to 800°C[12]. This is because of high thermal conductivity and strength which provides a unique feature of thermal shock resistant such as in bulletproof jackets (due to thermal expansion of B_4C)[13]. B_4C with small grain boundary impurities maintain their strength, appropriately underhigh-temperature condition (nearly 1500°C)[14]. Thus, B_4C has been selected as a reinforcement material.

Researchers have been preferred the use of different techniques for mixing the reinforcement with the treatment of Mg-matrix as composite materials[15,16]. Majoobi et al.[17] made Mg-MMC by varying reinforcing wt% of B_4C through the powder compaction technique and calculated the stress-strain properties. Their results reveal that the dynamic strength has been improved in comparison to pure Mg due to strengthening and heating. Rahamani et al.[18] fabricated Mg-MMCs with boron carbide by powder metallurgy. They investigated that the improved relative density under high loading indentation tests. Mohammadi et al.[19] studied on Mg-MMCs with the same reinforcement by

electromagnetic stir casting process has been used. Their results show high UTS of Mg-MMCs but affected at the high percentage of B_4C due to the formation of oxide films and porosity. Parizi et al.[20] also studied Mg-MMCs with graphene by extrusion process reveals improved tensile and compressive strengths. Their study shows uniform dispersions of graphene nano-particles but lower discontinuous precipitates cause strain failure. Patle et al.[21] used frictionstir processing to study the Mg alloy matrix with B_4C reinforcement to investigate the wear behaviour. Their result shows superior wear resistance and coefficient friction value at higher sliding velocity. Rezayatet al.[22] evaluated the tensile strength of Mg-based hybrid composite having B_4C and Zr as reinforcement. Their study reveals an increase in tensile strength with the addition of B_4C and proper interfacial bonding by Zr reinforcement.

Fabrication of Mg-based composites through stir casting route reveals improved results but still some modification required to make the Mg-based composites more ductile and wear-resistant. Hence, this paper deals with Mg-based B_4C reinforced composites by varying B_4C percentage need to be examined by an advanced SVSC process.

2 Experimental procedures

The squeezed vacuum-based stir casting (SVSC) process was used for the fabrication of Mg-based composites. Pure Mg ingots as base matrix and B_4C micro-particles (250μm) as reinforcement had been used for fabrication. The percentage distribution of boron carbide in Mg-matrix was shown in Table 1.

The two-step stir casting (SVSC) process was one of the modified methods of the ES technique. SVSC setup was integrated with muffle furnace, pressure regulator for vacuum, connectors for argon gas supply, bottom preheated runway, preheated hopper for reinforcement addition and attached MS mould to pour the melt (Fig. 1b). During continuous stirring, the matrix metal was placed in a vacuum-based preheated muffle furnace with a supply of argon with SF_6 cover gas to extinguish the fire. Then in a similar way tothe ES setup, the molten melt was stirred to attain a homogeneous arrangement. After that melt form of composite had been dropped into the mould by the bottom pouring approach. In the bottom pouring approach, a preheated small inclined runway was attached below the muffle furnace to maintain the temperature of the melt. Then the melt was poured into the mould and instantaneously squeeze pressure was applied by the hydraulic press for a few minutes to remove the residual defects. The working parameters had been explained in Table 2.

Table1 — Compositions of B_4C reinforced composites.

Composites Compositions	B_4C wt.%
Mg +0% B_4C	0
Mg+ 3% B_4C	3
Mg+ 5% B_4C	5
Mg+ 7% B_4C	7
Mg+ 9% B_4C	9

Table 2 — Process parameters for squeezed vacuum-based stir casting.

Parameters	Values set as
Stirring Temperature	750°C
Stirring Time	10 minutes
Stirring Speed	450 rpm
Protected cover gas pressure	2 bar
Preheat electric oven temperature	250°C
The bottom pouring furnace temperature	300°C
Squeeze pressure applied	250MPa

After solidifying, fabricated specimens had been taken out from the mould. The fabricated specimens were having dimensions of 250 mm in length and 45 mm in diameter. After that, specimens had been cut from the transverse direction in the dimensions of 10X10X10 mm^3 by a surface grinding machine for microstructural and hardness test. The metallographic studies of composites, worn surface and fractographic images had been analyzed in a metallurgical electron microscope (JMI, Central Instrumentation Facility, Delhi). A diffraction meter (JMI, Center of Nano science and Nanotechnology, Delhi) was tested for phase study of Mg-based composites up to 80 degrees at a speed of 2deg/min. The tensile test had been performed on a tensometer (JMI, ME Department, Delhi) at normal temperature with a transverse speed of 1m/sec. The tensile specimens had been prepared as per ASTM B557M–15 standards in dog-bone type shape[23]. The Rockwell hardness tests (JMI, ME Department, Delhi) had been performed on Rockwell hardness tester using a load of 100 kgf for 15 seconds and the average value of hardness were used for analysis purpose.

Abrasive wear tests had been operated using a wear testing apparatus i.e. Pin on Disc (DTU, Delhi, India) under 20N and 30N load and sliding speed of 5m/s.The dimensions of specimens were 50X10X10 mm^3 in a solid rectangular shape. All the specimens were rinsed with acetone before and after each of the test. An electronic balance was used for weighing the

specimens to 0.0001g of accuracy. The weight loss was used as a measure of wear. Electron microscopy was also used for abrasive wear study to wear mechanism analysis.

Thus in the present work, Mg-based B_4C reinforced compositeshad been developed by both SVSC and ES methods and analyzed the best-suited method for microstructural, tensile and wear results for these composites.

3 Results and Discussion

3.1 Microstructural analysis

The microscopic images of ES samples and SVSC samples were indicated in Fig. 2 under each of the same magnification. This indicates that the amalgamation of B_4C was more efficient in the SVSC process in comparison to ES. Figure 2(a-d) represents etched Mg-B_4C specimens' reveals non-dendritric eutectic structure (under 200µm magnification) and continuous Mg-matrix surface. Further, Fig. 2(a-d) represents the continuous and silvery zones were the primary Mg matrix and the other dark precipitates represent the eutectic regions having B_4C reinforcement. The dark precipitates become denser as the reinforced percentage of B_4C increases. However, Fig. 2 (a & b) shows protrude granules type boron carbide in the Mg-matrix. This was due to microstructural defects which cause the in homogeneous arrangement of B_4C reinforcement in the base matrix by the ES process. Whereas, Fig. 2 (c & d) showing proper and analogous amalgamation of B_4C-reinforced composites with the least porosity. This was due to suitable stirring parameters and instant squeezed pressure which causes appropriate inclusion of hard particulates of B_4C reinforcement in the Mg-based B_4C reinforced composites.

Although, B_4C (2.52 g/cm^3) was denser in comparison to Mg (1.74 g/cm^3) so B_4C try to analogous (not to homologous) in the composite melt, thus adequate processing parameters for composite melt was required[24]. Also, the melting temperature of Mg (650^{o}C) was lower than B_4C (the lowest amalgamation temperature for B_4C is 800-900 ^{o} C).So for the suitable blending of composite melt, melting temperature reaches upto 800-900 ^{o}C. This was possible by employing optimum stirring time, temperature and speed for the composite melt[25]. This developed in SVSC process. However, after amalgamation instant squeezed pressure was also applied in SVSC process which eliminates the maximum of its residual voids and oxides. Thus amalgamation of B_4C was more efficient in SVSC process in comparison to another process.

3.2 Diffraction analysis

The diffraction patterns of fabricated Mg-matrix and Mg-based B_4C reinforced composites were present in Fig. 3 (a) and (b-e). These patterns, reveals the variable peaks of Mg and B_4C at different intensities of the Mg-based composites. Each of the profiles of the composite specimens' reveals alpha-Mg as the highest peak due to the presence of the matrix material[26]. Fig. 3(b-e) shows alpha-Mg and beta-MgB_2 phases of B_4C reinforced composites. However other elements such as $B_{13}C_2$, and MgC_3were also present in Mg-matrix composites at different reinforcement percentage and diffraction angles. However, as the percentage of B_4C increases, the different peaks show variability at the same intensities.

3.3 Porosity analysis

Porosity can be considered as the measure of a number of defects that obstruct the improvement of strength in matrix composites. Porosity was inversely related to solidity and defined as the pores volume in percentage to the composite material total volume[27]. Porosity increases the fluid absorption present in the material but decreases its strength[28]. The results show the density of the B_4C-based composites was higher

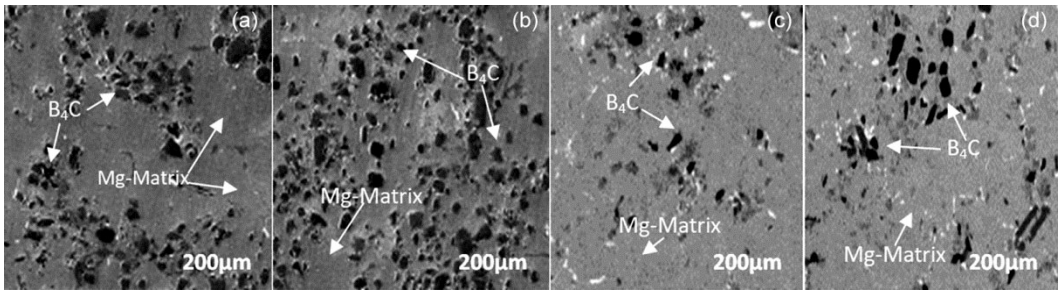

Fig. 2 — SEM Images of microstructures of fabricated specimens by different processes (a) 3wt% of B_4C Mg-Composite by electromagnetic stirring, (b) 9wt% of B_4C Mg-composite by electromagnetic stirring, (c) 3wt% of B_4C Mg-composite by SVSC, and (d) 9wt% of B_4C Mg-composite by SVSC.

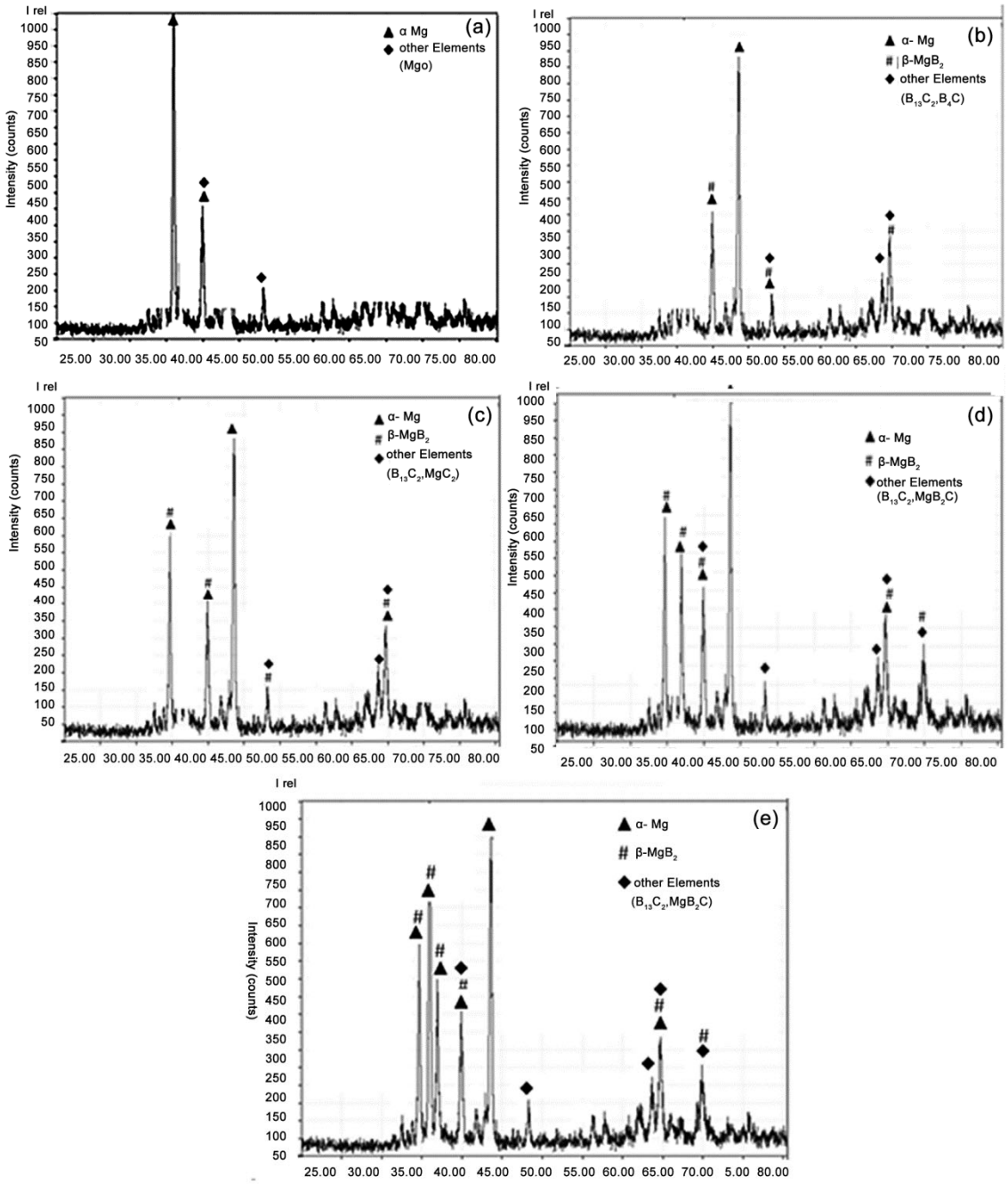

Fig. 3 — XRD Analysis of (a) Mg-Matrix, (b) Mg+3 wt. % B_4C, (c) Mg+5 wt. % B_4C, (d) Mg+7 wt. % B_4C, and (e) Mg+9 wt. % B_4C.

comparable to the density of Mg-matrix in both casting routes due to the addition of hard B_4C reinforcement. This can increase the porosity of B_4C reinforced composites. The B_4C-based specimen shows the slight higher porosity values for ES comparable to SVSC process route as shown in Fig. 4.

This was due to the proper drafting of stirring time and speed of the applied processing technique. And inadequate stirring time which maintains the whirling velocity of the melt which helps to regulate the particle distribution into the Mg-matrix[29]. Another possible reason for porosity formation was the inland oxides in the melt during solidification. The voids create the defect in the fabricated solid and cause porosity. This issue can be solved by providing high squeezed pressure which is possible by SVSC process. Therefore, SVSC process gave minimum the porosity formation and homogeneous distribution of

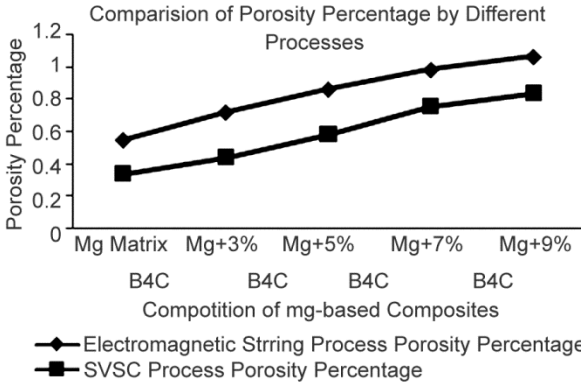

Fig. 4 — Porosity of Mg-based B_4C reinforced composites by both processes.

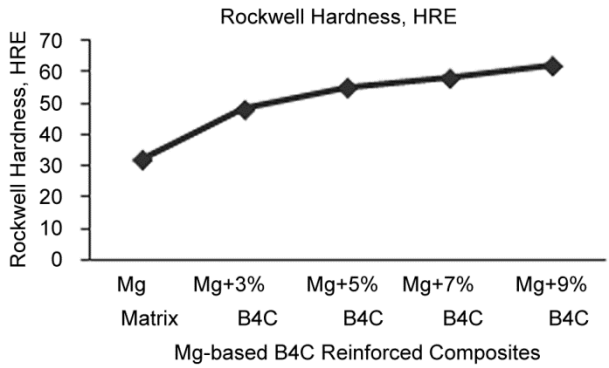

Fig. 5 — Hardness of Mg-based B_4C reinforced composites by SVSC processes.

Mg-based B_4C reinforced composites comparable to ES process.

The Mg-matrix and B_4C (3,5,7,9 wt%) reinforced composites by SVSC process shows 38% and 38-21% decrement of porosity percentage in comparison to Mg-matrix and B_4C reinforced composites by the ES process.

3.4 Rockwell hardness analysis

The hardness of the matrix and its composites were shown in Fig. 5. The hardness of the Mg-matrix was low while the hardness increases significantly with the addition of B_4C in Mg-based B_4C reinforced composites. This was because of the addition of B_4C hard reinforced particles which create an envelope over the Mg-matrix and offers resistance when the load was intended[30]. The hardness of B_4C reinforced composites was increased upto 33- 48% in comparison to Mg-matrix.

3.5 Tensile analysis

The tensile test had been conducted for both processing routes and three sets of each composite specimenare prepared for testing. In both processes, the tensile strength of Mg-matrix was the least whereas B_4C reinforced composites show higher tensile strength with the increase in the wt. percentage of B_4C as shown in Fig. 6. This was because of the addition of B_4C reinforcement shows a significant gain in strain hardening of the Mg-based B_4C reinforced composites and causes ductility to the composites[31]. Strain hardening was a desirable or undesirable strengthening of a composite material by plastic deformation[32]. This increment in strain hardening was more visible at higher wt. % of B_4C. But it gets affected at 9wt. % of B_4C due to the clustering of reinforced particles which causes composite brittle in nature. Clustering of reinforced

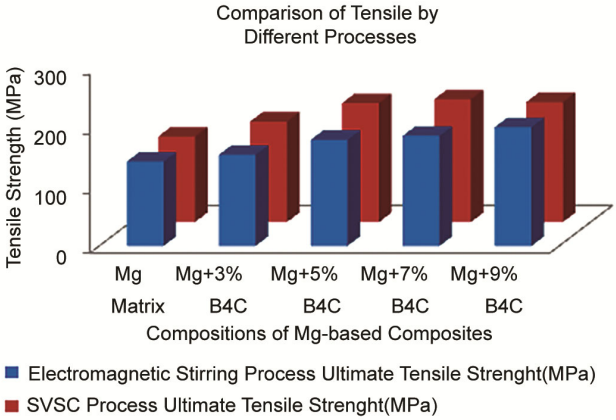

Fig. 6 — Tensile results of Mg-based B_4C reinforced composites by both processes.

particles generates hard carbide phases which initiate the localized cracks[33]. Thus the generation of localized interface cracks causes ductile to brittle transition in B_4C reinforced composites.

Figure 6 represents a high tensile strength of SVSC specimens as compared to an ES specimen. Mg-matrix and 9wt.% of B_4C reinforced SVSC composites shows the least increment (1-2%) in tensile strength as a comparison to the same percent of ES composites. However, 3-7wt.% of B_4C reinforced SVSC composites shows the highest increment (9-10%) in tensile strength as compared to the same percent of ES composites. From the analysis of images represent in Fig. 7 (a-d), it was found that with the increasing percentage of the reinforced particle, shows the formation of cleavage planes with micro-cracks and voids. This was due to the declination of ductility and initiation of a brittle fracture mechanism[34]. Although, fracture images of Fig. 7 (c, d) show micro voids for SVSC process. As micro-voids generates a transition phase (ductile to

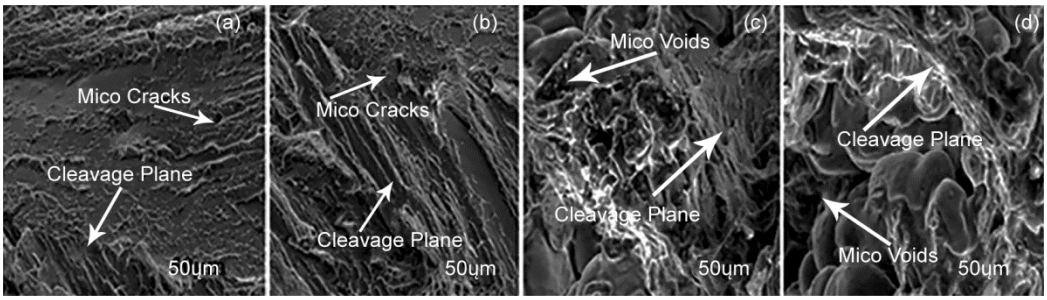

Fig. 7 — Microstructural Tensile Fracture Images of Fabricated Specimens by Different Processes (a) 3wt% of B_4C Mg-Composite by Electromagnetic Stirring, (b) 9wt% of B_4C Mg-composite by Electromagnetic Stirring, (c) 3wt% of B_4C Mg-composite by SVSC, and (d) 9wt% of B_4C Mg-composite by SVSC.

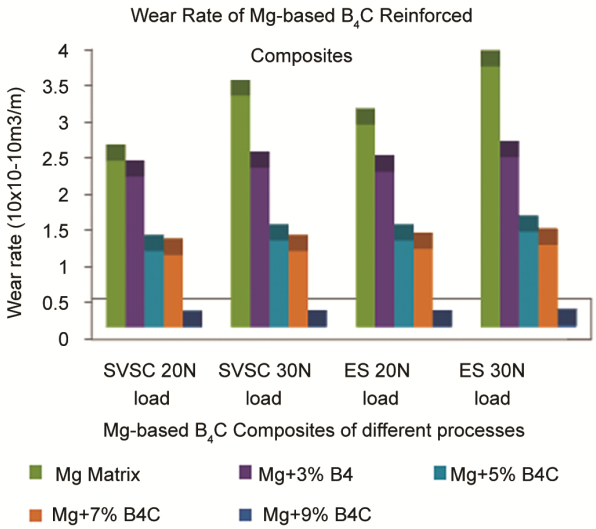

Fig. 8 — Wear Rate of Mg-based B_4C Reinforced Composites at 20N and 30N load by SVSC and Electromagnetic Stirring (ES) Processes.

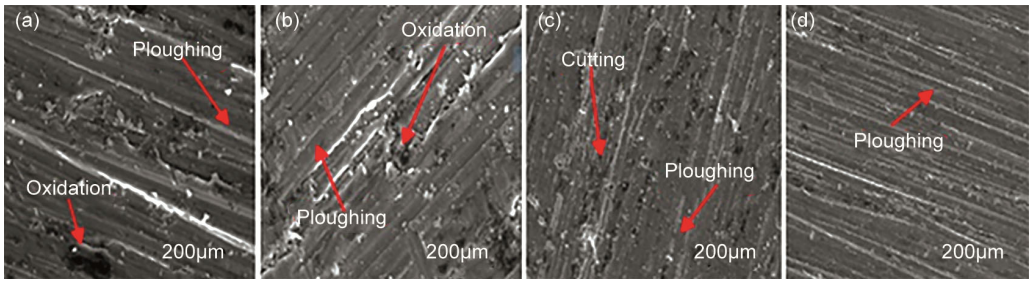

Fig. 9 — SEM Images of Microstructures of Fabricated Specimens by SVSC Process (a) 3wt% of B_4C Mg-Composite at 10N, (b) 9wt% of B_4C Mg-composite at 20N, (c) 3wt% of B_4C Mg-composite at 10N, and (d) 9wt% of B_4C Mg composite at 20N.

brittle) of interfacial planes in the Mg-based B_4C reinforced composites.

3.6 Wear rate analysis

The abrasive wear of Mg-matrix and their composites (Fig. 8) were carried out at the load of 20N and 30N with a fixed sliding distance and speed. This investigation reveals that the rate of wear decreases with an increase in wt. % of boron carbide due to the high hardness of the Mg-based B_4C reinforced composites. The abrasive wear rate of Mg-matrix was higher at each load as compared to their composites. This was due to the soft nature of Mg-matrix cause's increase in depth of penetration of the matrix with the increase in the load[35]. The abrasive wear results show 17% and 11 % decrement in abrasive wear rate of SVSC Mg-matrix at 20 and 30 N load respectively in comparisons to ES Mg-matrix.

Figure 9 (a-d) shows the worn images of Mg-based B_4C composites. These images were used to identify the abrasive wear and material removal mechanisms in the composites and Mg-matrix. From the analysis of the images, it was found that with the increase in load the grooves become wider as compared to lower load. The main material removal mechanism in the Mg-matrix was mainly ploughing. The ploughing mechanism was due to the abrasion heating between the disc and the pinned specimen[36]. This result to the formation of the oxide layer (because of the oxidative nature of Mg) and with the repetitive rubbing action induces the deterioration of the oxide layer in the form of wear debris.

However, the wear rate also occurs due to high porosity. The high porosity indicates inhomogeneous grain formation in the composite which creates lumps of particulates[37]. As these lumps activate the microstructural defects such as oxides and voids. The presence of oxides and voids was an indication of oxidative nature of the composite. Thus dark pits of oxides were the form of oxidation wear mechanism[38]. Thus, ES composites show greater wear rate than SVSC composites as shown in Fig. 9 (a, b).

4 Conclusions

The following outcomes have been drawn from the present research work:

- Successful fabrication of Mg-based B_4C reinforced composites have been done through electromagnetic stirring (ES) and squeezed in vacuum-based stir casting (SVSC).
- Both processes contribute uniform distribution but SVSC process shows a homogeneous amalgamation of boron carbide particles with minimum voids and porosity through microscopic images.
- The porosity formation has been higher in the ES processed composites due to improper mixing turbulence of stirrer and inappropriate vacuum atmosphere as compared to SVSC processed composites. SVSC composites consist of 9 wt. % of B_4C show 21% of reduction as compared to the same composition of ES composite.
- The hardness of Mg-based B_4C reinforced composites has been higher (about 33-48%) in comparison to Mg-matrix due to the addition of hard reinforced boron carbide particulates.
- A 3-7 wt. % of B_4C reinforced SVSC composites show the 9-10% increment in tensile strength as compared to the same composition of ES composites. Whereas, Mg-matrix having 9 wt. % of B_4C composite reveals the least tensile strength.
- Further, the fractured images show cleavage planes, microvoids and cracks due to declination of ductility and initiation of a brittle transition phase as the B_4C percentage increases.
- SVSC composites consist of 9 wt.% of B_4C showthe reduction of wear rate upto 58% and 66% at 20N and 30N load respectively as compared to ES composites due to an adequate amalgamation of hard reinforced particles in Mg-based B_4C reinforced composites.
- Although, worn images show oxidation and ploughing mechanism with the increase in load and depth of penetration in Mg-matrix B_4C reinforced composites in both processes.

References

1 Tekumalla S & Gupta M, *Nanosci Nanotechnol Adv Compos*, (2019) 3.
2 Gialanella S & Malandruccolo A, *Aero Ally*, (2020) 41.
3 Wendt A, Weiss K, Ben-Dov A, Bamberger M & Bronfin B, *Ess Mg Technol*, (2016) 65.
4 Rathee S, Maheshwari S & Siddiquee A N, *Mater Manuf Process*, 33 (2018) 239.
5 Suneesh E & Sivapragash M, *Mater Manuf Process*, 33 (2018) 1324.
6 Tokunaga T, Ohno M & Matsuura K, *J Mater Sci Tech*, 34 (2018) 1119.
7 Crivello J C, Dam B, Denys R V, Dornheim M, Grant D M, Huot J & Milčius D, *App Phy A*, 122 (2016) 97.
8 Ramanathan A, Krishnan P K & Muraliraja R, *J Manuf Process*, 42 (2019) 213.
9 Kumar S D, Ravichandran M, Meignanamoorthy M, Sakthivelu S, Alagarsamy S V & Chanakyan C, *Mater T Proc*, (2020).
10 Jabbari A H & Sedighi M, *Int J Met Cast*, (2019) 1.
11 Ebrahimi S, Heydari M S, Baharvandi H R & Ehsani N, *Int J Ref Met Hard Mater*, 57(2016) 78.
12 Kumar A & Rai R N, *IOP Conf Ser: Mater Sci Engg*, 377 (2018) 012092.
13 Rasim K, Ramlau R, Leithe-Jasper A, Mori T, Burkhardt U, Borrmann H & Grin Y, *Angewand Chemie*, 130 (2018) 6238.
14 Pascale S, Scatena E, Fabbri F & Cataldo F, *Full, Nanotub Carbon Nanostr*, 25 (2017) 585.
15 Meher A, Mahapatra M M, Samal P, Vundavilli P R & Madavan S P, *Mater T Proc*,18 (2019) 4034.
16 Kandpal B C, Kumar J & Singh H, *Mater T Proc,* 5 (2018) 5.
17 Majzoobi G H & Rahmani K, *Int J Min Metallur Mater*, 27 (2020) 252.
18 Rahmani K & Majzoobi G H, *J Compos Mater*, (2019).
19 Mohammadi H, Emamy M & Hamnabard Z, *Int J Met Cast*, (2019) 1.
20 Parizi M T, Ebrahimi G R & Ezatpour H R, *Mater Sci Engg: A*, 742 (2019) 373.
21 Patle H, Sunil B R & Dumpala R, *Mater Res Exp*, *7*(2020) 016586.
22 Rezayat M, Bahremand M R, Parsa M H, Mirzadeh H & Cabrera J M, *J Ally Comp*, 685 (2016) 70.

23 Vanli A S & Akdogan A, *Ind J Engg Mater Sci,* 6 (2019) 27.
24 Reddy K M, Guo J J, Shinoda Y, Fujita T, Hirata A, Singh J P & Chen M W, *Nat Comm,* 3 (2012) 1.
25 Maurya M, Kumar S, Bajpai V & Kumar M N, *Mater Test*, 62 (2020) 196.
26 Turan M E, Sun Y, Akgul Y, Turen Y & Ahlatci H, *J Ally Comp*, 724(2017) 14.
27 Vahid A, Hodgson P & Yuncang L, *J Ally Comp*, 724 (2017) 176.
28 Purohit R, Dewang Y, Rana R S, Koli D & Dwivedi S, *Mater T Proc*, 5 (2018) 6009.
29 Moona G, Walia R S, Rastogi V & Sharma R, *Mater Res Exp*, 6 (2019) 1165d5.
30 Li X, Jiang D, Zhang J, Zhu Y, Chen Z & Huang Z, *Int J App Cer Tech*, 13 (2016) 584.
31 Wu P D, Guo X Q, Qiao H, Agnew S R, Lloyd D J & Embury J D, *Acta Mater*, 122 (2017) 369.
32 Abbas A & Huang S J, *Mater Sci Engg: A*, *780* (2020)139211.
33 Seenuvasaperumal P, Elayaperumal A & Jayavel R, *Tri Int*, 111 (2017) 18.
34 Dastgerdi J N, Marquis G, Anbarlooie B, Sankaranarayanan S & Gupta M, *Compos Struc*, 142 (2016) 130.
35 Kaushik N, Sri C C & Rao R N, *Proc Inst Mech Eng Part J: J Engg Trib*, 232 (2018) 672.
36 Singh A & Niraj B, *Mater Res Exp*, 6 (2019).
37 Aydin F, Sun Y, Ahlatci H & Turen Y, *Trans Ind Inst Met*, 71 (2018) 873.
38 Dey A & Pandey K M, *Int J Mater Res*, 109 (2018) 1050.